STRUCTURAL CHARACTERIZATION AND REACTIVITY STUDIES OF SEVERAL TRIRUTHENIUM CARBONYL CLUSTER COMPLEXES MEDIATED VIA P–C/As–C BOND CLEAVAGE AND C–H BOND ACTIVATION

SITI SYAIDA BINTI SIRAT

UNIVERSITI SAINS MALAYSIA

2018

STRUCTURAL CHARACTERIZATION AND REACTIVITY STUDIES OF SEVERAL TRIRUTHENIUM CARBONYL CLUSTER COMPLEXES MEDIATED VIA P–C/As–C BOND CLEAVAGE AND C–H BOND ACTIVATION

by

SITI SYAIDA BINTI SIRAT

**Thesis submitted in fulfillment of the requirements
for the Degree of
Doctor of Philosophy**

December 2018

ACKNOWLEDGEMENT

TABLE OF CONTENTS

LIST OF TABLES

LIST OF FIGURES

LIST OF SCHEMES

LIST OF ABBREVIATIONS AND SYMBOLS

Å	angstrom
a, b, c	unit cell dimensions
α, β, γ	unit cell angles
atm	standard atmosphere
As	arsine
Av	average
Bi	bismuth
Bma	2,3-bis(diphenylphosphino)maleic anhydride
Bpcbd	1,2-bis(diphenylphosphino)cyclobutenedione
Bu^n	n-butyl $-CH_2CH_2CH_2CH_3$
Bu^t	tert-butyl $-C(CH_3)_3$
°C	degrees centigrade (Celcius)
^{13}C	carbon
calc.	calculated
cm	centimetre (10^{-2} m)
cm^3	cubic centimetre (millilitre; 10^{-6} m^3)
CO	carbonyl
Cy	cyclohexyl (C_6H_{11})
d	doublet
δ	chemical shift
°	degree (angle)
dd	doublet of doublet
dcpm	1,1-bis(dicyclohexylphosphino)methane
decomp.	decompose

diop   4,5-bis(diphenylphosphinomethyl)-2,2-dimethyl- 1,3-dioxolane

dmpm   bis(dimethylphosphino)methane ($Me_2CH_2PMe_2$)

DPB   1,4-bis(diphenylphoshino)benzene ($Ph_2P(C_6H_4)PPh_2$)

dpam   1,1-bis(diphenylarsino)methane ($Ph_2AsCH_2Ph_2$)

dpmb   1,2-bis[(diphenylphosphino)methyl]benzene

dppa   bis(diphenylphosphino)acetylene ($Ph_2PC{\equiv}CPPh_2$)

dppb   1,4-bis(diphenylphosphino)butane ($Ph_2P(CH_2)_4PPh_2$)

dppe   1,2 bis(diphenylphosphino)ethane ($Ph_2P(CH_2)_2PPh_2$)

dppf   l,l-bis(diphenylphosphino)ferrocene ($Ph_2P(C_5H_4)Fe(C_5H_4)PPh_2$)

dpph   1,6-bis(diphenylphosphino)hexane ($Ph_2P(CH_2)_6PPh_2$)

dppm   1,2 bis(diphenylphosphino)methane ($Ph_2PCH_2PPh_2$)

dppp   1,3-bis(diphenylphosphino)propane ($Ph_2P(CH_2)_3PPh_2$)

dpppe   1,5-bis(diphenylphosphino)pentane ($Ph_2P(CH_2)_5PPh_2$)

dppee   vinylidenebis(diphenylphosphine) ($Ph_2P)CH=CH(PPh_2$)

Et   ethyl ($-CH_2CH_3$)

Fc   ferrocenyl ($C_5H_4)Fe(C_5H_5$)

Fc'   ferrocenyl ($C_5H_4)Fe(C_5H_4$)

F-dppe   1,2-bis(pentafluorophenylphosphino)ethane

ffars   1,2-bis(dimethylarsino)-3,3,4,4-tetrafluorocylobutene

^{1}H   proton

h   hour

η   eta

Hz   Hertz

IR   infra-red

J   coupling constant

L'	general monodentate phosphine or arsine
L-L	general bidentate phosphine or arsine
M	general transition metal
m	multiplet
mapm	bis(di(o-N-methylanilinyl)phosphino)methane
m.p.	melting point
μ	bridging bonding mode
Me	methyl (-CH_3)
mg	milligram
MHz	megahertz (10^6 Hz)
min	minute
ml	millilitre
mmol	millimole
N	nitrogen
Na[Ph_2CO]	sodium benzophenone ketyl
NMR	Nuclear Magnetic Resonance
P	phosphorus
^{31}P	phosphorus-31
Ph	phenyl (C_6H_5)
ppm	parts per million
PPN$^+$	bis(triphenylphosphino) iminium ($Ph_3P)_2N^+$
^{n}Pr	n-propyl (-$CH_2CH_2CH_3$)
^{i}Pr	iso-propyl (-$CH(CH_3)_2$
PTh$_3$	tris(2-thienyl)phosphine
R	aryl

R_w	weighted residual
s	singlet
Sb	stibine
t	triplet
THF	tetrahydrofuran
TLC	thin layer chromatography
V	unit cell volume
Z	number of molecules in a unit cell

KAJIAN PENCIRIAN STRUKTUR DAN KEREAKTIFAN BEBERAPA KOMPLEKS GUGUSAN KARBONIL TRIRUTHENIUM MELALUI PENGANTARAAN PEMUTUSAN IKATAN P–C/As–C DAN PENGAKTIFAN IKATAN C–H

ABSTRAK

Perkembangan gugusan logam karbonil yang melibatkan transformasi ligan kumpulan 15 terus menjadi bidang penyelidikan aktif. Maka, minat kajian terhadap tindakbalas termolisis ke atas kompleks gugusan karbonil triruthenium yang mengandungi difosfin dengan rantai karbon bertulang belakang panjang [1,3-bis(difenilfosfino)propana (dppp) dan 1,4-bis(difenilfosfino)butana (dppb)]; adalah menjangkakan bahawa kemasukan difosfin yang mengandungi lebih daripada satu karbon bertulang belakang metilena akan sacara radikal mengubah reaktiviti seterusnya menghasilkan produk tindakbalas baharu. Siri $Ru_3(CO)_{10}$(L-L), $[Ru_3(CO)_{11}]_2$(L-L) [di mana 1,3-bis(difenilfosfino)propana (dppp), 1,4-bis(difenilfosfino)butana (dppb), 1,5-bis(difenilfosfino)pentana (dpppe) and 1,6-bis(difenilfosfino)hexana (dpph)], $Ru_3(CO)_8$(L-L] [di mana L-L = 1,1-bis(difenilarsino)metana (dpam)] dan $Ru_3(CO)_9$(μ-dppb)(L') [di mana L' = PPh_3 dan $AsPh_3$] dihasilkan melalui tindakbalas penukargantian yang dimulakan oleh Na[Ph_2CO] dan kaedah termal. Kepelbagaian panjang ikatan Ru–Ru di $Ru_3(CO)_{10}$(L-L) ditemukan adalah berkaitan dengan sudut intrasiklik logam-logam-ligan [Ru–Ru–P]. Dua puluh lapan kompleks telah dicirikan menggunakan teknik analisis dan spektroskopi. Dua puluh satu daripadanya telah dicirikan struktur menggunakan pembelauan hablur tunggal kristalografi sinar-X. Kajian ini menunjukkan bahawa

implikasi difosfin dengan rantai karbon bertulang belakang panjang [dppp dan dppb] terhadap gugusan Ru_3 adalah lebih labil daripada 1,1-bis(difenilfosfino)metana (dppm) dan 1,2-bis(difenilfosfino)etana (dppe) untuk tindakbalas selanjutnya. Kereaktifannya berjaya menyediakan beberapa jenis kompleks yang belum pernah terjadi sebelum ini melalui pemutusaan ikatan C–P/As dan pengaktifan ikatan C–H. Ligan dppm dan dpam cenderung untuk memelihara integriti teras Ru_3 semasa tindakbalas termolisis.

STRUCTURAL CHARACTERIZATION AND REACTIVITY STUDIES OF SEVERAL TRIRUTHENIUM CARBONYL CLUSTER COMPLEXES MEDIATED VIA P–C/As–C BOND CLEAVAGE AND C–H BOND ACTIVATION

ABSTRACT

The development of metal carbonyl cluster mediated Group 15 ligand transformations continues to be an area of active research. It is therefore of considerable interest to investigate the thermolysis reactions of triruthenium carbonyl cluster complexes containing diphosphines with long chain carbon backbone [1,3-bis(diphenylphosphino)propane (dppp) and 1,4-bis(diphenylphosphino)butane (dppb)]; anticipating that the introduction of more than one methylene carbon backbone of diphosphine ligands would radically alter its reactivity leading to new reaction products. Series of $Ru_3(CO)_{10}(L\text{-}L)$, $[Ru_3(CO)_{11}]_2(L\text{-}L)$ [where L-L = 1,3-bis(diphenylphosphino)propane (dppp), 1,4-bis(diphenylphosphino)butane (dppb), 1,5-bis(diphenylphosphino)pentane (dpppe) and 1,6-bis(diphenylphosphino)hexane (dpph)], $Ru_3(CO)_8(L\text{-}L)$] [where L-L = 1,1-bis(diphenylarsino)methane (dpam)] and $Ru_3(CO)_9(\mu\text{-}dppb)(L')$ [where L' = PPh_3 and $AsPh_3$] were prepared by substitution reactions initiated by $Na[Ph_2CO]$ and thermal method. The variation of Ru-Ru bond lengths in $Ru_3(CO)_{10}(L\text{-}L)$ were found to be related with intracyclic metal-metal-ligand [Ru–Ru–P] angles. Twenty-eight complexes have been prepared and characterized by spectroscopic and analytical techniques. Twenty-one of these have been structurally characterized by using single crystal X-ray crystallography. This study has demonstrated that diphosphine with long chain carbon backbone ligands

[dppp and dppb] on Ru_3 clusters are more facile than 1,1-bis(diphenylphosphino)methane (dppm) and 1,2-bis(diphenylphosphino)ethane (dppe) for further reactions. Its reactivity was used to successfully prepare some unprecedented type of complexes via C–P/As bond cleavage and C–H bond activation. The dppm and dpam ligands tend to preserve the integrity of the Ru_3 core during thermolysis reactions.

CHAPTER 1

INTRODUCTION

1.1   Transition metal carbonyl cluster chemistry

Transition metal carbonyl cluster chemistry can be considered to lie at the interface between conventional organic and inorganic chemistry since it involves the interaction between inorganic metal ions and organic molecules. This area of chemistry deals with transition metals in Groups 7-10 to form clusters with π-acceptor ligands, especially the carbonyl (CO) ligand [1]. The CO has lone electron pairs on both the carbon and oxygen atoms. The *sp* orbital of the carbon atom containing its lone electron pair can overlap with a metal hybrid orbital. The bonding of CO to a transition metal centre involves the donation of electron pair from the ligand to the metal atom through a σ-donation. This bond is complemented by a second bond, (π-back bonding), where a filled metal *d* orbital containing an electron pair can overlap with an empty π^* antibonding orbital of the CO ligand (Figure 1.1). Since CO is only a weak σ-donor ligand, the metal-to-ligand (d-π^*) interaction provides an important contribution to the stability of the M-CO bond [2].
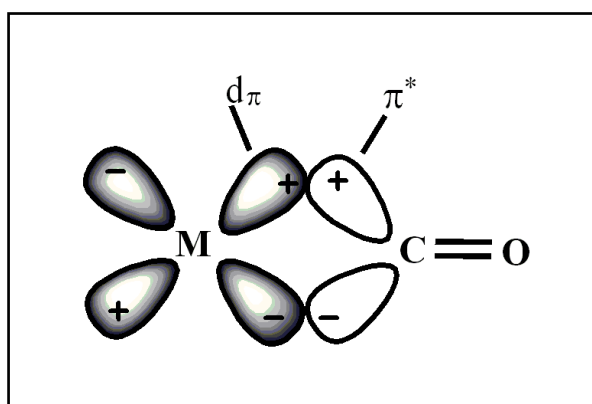
Figure 1.1   Bonding of CO to a metal atom. The overlap between a filled metal d_π orbital and an empty CO π^* orbital to give the π component of the M-CO bond [3].

1

Metal cluster complexes are defined as compounds that contain two or more metal atoms that are held together by direct metal-metal bonds [4]. A metal triangle is the simplest ring of metal atoms in metal cluster chemistry. It can be used to construct the metal cluster of higher nuclearity by sharing edges or vertices and can be stacked either directly on top of each other or with other metal atoms between pairs of triangles [5]. Most studies of cluster chemistry have gone beyond the determination of molecular structure with the application towards areas of catalysis. The metal cluster has a considerable advantage over mononuclear complexes in modelling of metal surface reactivity because they possess a variety of spatial arrangements of coordination sites [1]. In fact, the function of a metal-metal framework is to facilitate the coordination of the ancillary ligands to more than one metal centre that is not accessible to mononuclear species [6].

Historically, transition metal carbonyl, $Ni(CO)_4$ which was first synthesized by Ludwig Mond in 1884, is the first known binary metal carbonyl complex, prepared from the reaction of Ni powder with CO [7]. Since the discoveries of $Ni(CO)_4$, similar reactions led to the preparation of $Fe(CO)_5$ and $Fe_2(CO)_9$ [8]. Following this interest, the first metal cluster carbonyl complex, $Fe_3(CO)_{12}$ was synthesized by the thermal decomposition of $Fe_2(CO)_9$ [9]. In 1910, the first ruthenium carbonyl complex $(Ru_3(CO)_{12})$ was isolated from the reaction of ruthenium metal with CO at 300 °C and 400 atm [10] but it was not correctly formulated until an X-ray crystallographic analysis was performed in 1961 [11]. The improvements of methods of preparation have been reported frequently and the best quantitative conversion of hydrated ruthenium trichloride to $Ru_3(CO)_{12}$ was from the carbonylation of a 1 % methanol solution (50-60 atm CO, 125 °C, 16-18 h). In the case of $Os_3(CO)_{12}$, Manchot and co-workers originally reported it as $Os_2(CO)_9$ and later the trimetallic formulation

$Os_3(CO)_{12}$ was established [12]. The synthesis of $Os_3(CO)_{12}$ has been developed starting from the reaction of OsO_4 with CO in xylene (128 atm, 175 °C) [13] and an improved low-pressure synthesis has been introduced in EtOH for better yield [14].

The structures of $Ru_3(CO)_{12}$ and $Os_3(CO)_{12}$ form a triangle and four terminal carbonyls on each metal centre, two being at axial and two equatorial positions. The structure of $Fe_3(CO)_{12}$ differs from that of $Ru_3(CO)_{12}$ and $Os_3(CO)_{12}$ because two bridging carbonyl ligands are coordinated along one Fe–Fe edge with the remaining ten carbonyl groups are in the terminal positions. The Group 8 binary metal carbonyl cluster is shown in Figure 1.2. Structural data for $Fe_3(CO)_{12}$, $Ru_3(CO)_{12}$ and $Os_3(CO)_{12}$ are summarized in Table 1.1.
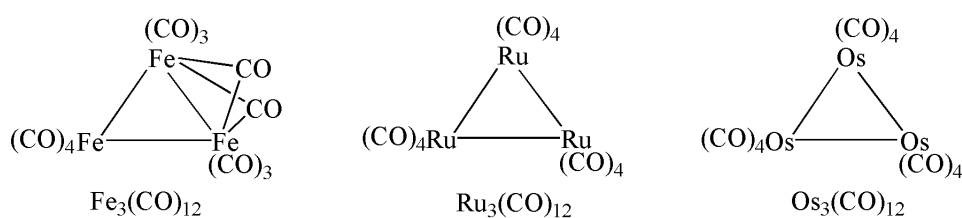
Figure 1.2   Group 8 binary metal carbonyl cluster.

Table 1.1   Average bond lengths and bond angles for $Fe_3(CO)_{12}$, $Ru_3(CO)_{12}$ and $Os_3(CO)_{12}$.

	$Fe_3(CO)_{12}$	$Ru_3(CO)_{12}$	$Os_3(CO)_{12}$
Av. M-M (Å)	2.639(3)	2.854 (4)	2.8771 (27)
Av. M-C (axial) (Å)	1.83	1.942 (4)	1.946 (6)
Av. M-C (equatorial) (Å)	1.815	1.921 (5)	1.912 (7)
Av. M-C (bridging) (Å)	2.0525	-	-
Av. C-O (axial) (Å)	1.1425	1.133 (2)	1.134 (8)
Av. C-O (equatorial) (Å)	1.1217	1.127 (2)	1.145 5)
Av. Within the M_3 triangle (°)	60.0	60.0 (1)	60.0
Av. M-C-O (axial) (°)	173.0	172.98	175.3167
Av. M-C-O (equatorial) (°)	173.0	178.91	178.3667
Av. M-C-O (bridging) (°)	148	-	-

The average of Ru–Ru bond length is slightly shorter than Os–Os bond lengths which are related to the energy absorption in the electronic spectra. The lowest energy absorption in the electronic spectra of $[M_3(CO)_{12}]$ (M=Fe, Ru, Os) is in the order Os >Ru >Fe and may reflect increasing M–M bond strengths in the Ru and Os clusters [15]. The equatorial angles of M–C–O moieties are almost linear although there is a tendency for the axial angles of M–C–O moieties to distort due to van der Waals repulsions between axial oxygen atoms [16]. The strength of Ru–Ru in $Ru_3(CO)_{12}$, when compared with the Fe_3 cluster in $Fe_3(CO)_{12}$, can be verified by most of the reactions of the ruthenium complex, which often afford products retaining the cluster. In contrast, the simple substitution reactions of $Fe_3(CO)_{12}$ cluster with tertiary phosphines produce mononuclear complexes [17].

The chemistry of clusters carrying a ligand other than carbonyl continues receiving attention from several research groups [18-21]. This breakthrough turned out to be quite outstanding since for a long time it was believed that ligands may act as ancillary ligands to stabilise and affect the reactivity of the cluster [1]. The ligand substitutions chemistry of metal carbonyl cluster is not only of academic interest but also of standing in providing a detailed description on their applications in catalysis and their reactivity.

1.2   Group 15 ligands

(N), (P), (As), (Sb) and (Bi) comprise the representative group 15 elements. The chemistry of nitrogen is different from the other group 15 elements since nitrogen readily forms double bond [22]. The interesting chemistry of metal-group 15 clusters may be related to the element characteristic ranging from the non-metallic (N and P) through metalloid (As and Sb) to metallic (Bi) [23]. However, handling some of group

15 ligands is difficult. Many Group 15 elements as they are pyrophoric, sensitive to air oxidation and malodorous [24]. In fact, there is a general lack of readily available commercial group 15 ligands especially arsine, stibine as well as bismuth.

Among all the elements concerned, phosphorus has continued to play a major role in transition metal (*d*-block) coordination and organometallic chemistry [25, 26]. The tertiary phosphines have stabilized low oxidation states of metal centres, metal-hydrogen, metal-carbon, and metal-olefin bonds [27]. They also can be used to modify both the electronic and steric properties of their corresponding derived coordination compounds by varying the substituent groups on the phosphorus (R on PR_3) in a systematic fashion [24]. As a result, the activity, selectivity, and stability of a catalytic system can be tuned via electronic and/or steric considerations [24]. The number of known tertiary phosphine ligands is truly immense and includes examples of monodentate as well as a great variety of substituents on phosphorus. There are two important factors involved in the coordination of tertiary phosphine ligands with transition metal atoms. First, the electronic character of the M–P bond results from combination of the σ bond formed by donation of the lone pair electron from the P to the M atom and back donation towards the P ligand to accept electron density from the $3d$ metal orbitals into the empty σ* orbitals of the P atom. The second factor controlling the coordination of a ligand is the steric effect associated with the size of the ligand [28]. The steric effect also known as the Tolman cone angle was introduced by Tolman through a measurement size of the cone angle of the monodentate phosphine ligands. The cone angle (θ) describes the opening angle of the cone that just touches the surface of the outermost atoms of a phosphine ligand. The apex of the cone is positioned at the central metal atom, with a settled metal–phosphorus bond length of 2.28 Å as showed in Figure 1.3 [29].
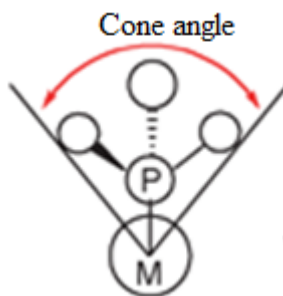
Figure 1.3   The cone angle proposed by Tolman [29].

Nowadays, the cone angle is still a matter of discussion and widely used to describe the bulkiness of ligands. This model has been extended to cover the other Group 15 elements namely, As, Sb and Bi. The electronic effects can be defined as a result of transmission along chemical bonds and the phosphorus ligands can be ranked in an electronic series based on CO stretching frequency of the trans carbonyl group in Ni(0) complexes of the general formula $Ni(CO)_3L$ [where L = monodentate Group 15 ligand] in CH_2Cl_2 [29]. The electronic effects together with steric effects have at times been invoked to explain the influence of different ligand substituents on coordination with transition metal and there are also advances in improving Tolman's Cone Angle and electronic parameter [30-32]. This concept can also be applied for ditertiary phosphine ligands by approximating their cone via the cones of substituents and the angle between the metal–phosphorus bond and the half angle of P–M–P (bite angle) [31, 33, 34].

The ditertiary phosphine ligand also known as bidentate phosphine ligand. The most common bidentate phosphine ligands are found linked to a backbone unit [-$(CH_2)n$-, -C_6H_4-, -CH=CH- and -$(C_5H_4)Fe(C_5H_4)$-] between two tertiary phosphines. Such bidentate phosphines can adopt a variety of bonding modes on the Group 8 metal

cluster. These bidentate phosphines can act as a monodentate ligand, chelating a single metal, bridging across a metal-metal bond and linking across two clusters. The reactivity of phosphine ligands with metal carbonyl cluster have been established with respect to the coordination modes adopted by these ligands [35, 36]. In addition, the effect of the methylene chain length of the bidentate phosphine ligand on coordination modes of metal carbonyl cluster has been studied for trinuclear ruthenium [36] and osmium clusters [37, 38]. From these studies, the chelating tendency of $Ph_2P(CH_2)_nPPh_2$ ligands decreases as the chain length increases, with the inclination to chelate greatest when n = 2 [37]. Overall, a wide range of clusters with simple terminal [39, 40], edge-bridged [41, 42] and face-capped [43, 44] phosphine ligands have been prepared from the reaction of phosphines with metal clusters.

1.3 Synthesis and structures of some triruthenium and phosphine and arsine complexes

Early studies on the reactions of $Ru_3(CO)_{12}$ with phosphines or arsines were commonly performed by thermal or photochemical methods. The irradiation of $Ru_3(CO)_{12}$ and PPh_3 in hexane gives $Ru(CO)_4(PPh_3)$ and $Ru(CO)_3(PPh_3)_2$ as the major products with very low yields of $Ru_3(CO)_{11}(PPh_3)$ [45]. The mono- and disubstituted products can also be obtained from thermal reactions though the trisubstituted complexes often predominate if chromatographic separation is employed to treat the reaction products rather than crystallization [46]. The thermal reaction of $Ru_3(CO)_{12}$ with PR_3 (R = Ph, Et, Bu^n, OPh) in general leads to derivatives of $[Ru_3(CO)_{11}(PR_3)]$, $[Ru_3(CO)_{10}(PR_3)_2]$ and $[Ru_3(CO)_9(PR_3)_3]$ [46]. A ligand transfer reaction between low-valent platinum tertiary phosphines complexes and $Ru_3(CO)_{12}$ has also been used to produce mono- and disubstituted $Ru_3(CO)_{12}$ complexes [47].

In the early 1980's a new method to prepare mono-, di- and trisubstituted cluster products from the parent cluster $Ru_3(CO)_{12}$ was successfully demonstrated by using sodium benzophenone ketyl $Na[Ph_2CO]$ to induce specific carbonyl substitution of metal clusters [48]. This method was developed by M. I. Bruce and co-workers after Bezems et al. [49] and Rieger et al. [50] first showed that specific CO substitution in metal carbonyl complexes can be electronically induced in mononuclear complexes. The proposed mechanism for the $Na[Ph_2CO]$ method involves an electron transfer catalysed (ETC) process and the mechanism is showed in Scheme 1.1.

$$Ru_3(CO)_{12}$$

$$+ \quad [Ph_2CO]^{\bullet-}$$

$$Ru_3(CO)_{11}L \qquad [Ru_3(CO)_{12}]^{\bullet-} \quad + \quad Ph_2CO$$

$$L$$

$$Ru_3(CO)_{12} \qquad [Ru_3CO)_{11}L]^{\bullet-} \qquad CO$$
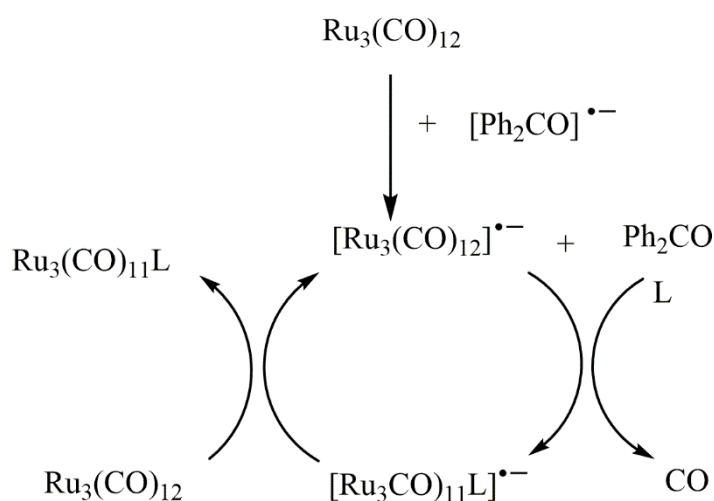
Scheme 1.1   Catalytic cycle of benzophenone ketyl
radical anion reaction mechanism [48].

Addition of $Na[Ph_2CO]$ to a solution of $Ru_3(CO)_{12}$ results in electron transfer from the ketyl radical anion to the cluster. Presumably, the Ru–Ru bond cleavage occurs to generate a labile 17 electron metal centre; related mononuclear 17 electron carbonyls are very readily substituted. The substituted cluster radical anion is less stable than that formed by the carbonyl and rapid electron transfer to unreacted cluster carbonyl establishes a cycle that is followed until either carbonyl or ligand is used up. Besides, there are two characteristics that should be met for the $Na[Ph_2CO]$ reaction

to occur: (1) the cluster carbonyl should be reduced without fragmentation and the resulting anion must have a long enough lifetime for substitution to take place; (2) to facilitate the electron transfer from the substituted radical anion to the substituted one and the substituting ligand must be a better Lewis base than the CO ligand [48]. However, the Na[Ph$_2$CO] method was not successful for synthesizing trisubstituted complex with sterically demanding phosphine ligands, such as PCy$_3$. The reactions of Ru$_3$(CO)$_{12}$ between PCy$_3$ with the presence of Na[Ph$_2$CO] only successfully gave Ru$_3$(CO)$_{11}$(PCy$_3$) and Ru$_3$(CO)$_{10}$(PCy$_3$)$_2$ complexes, but no Ru$_3$(CO)$_9$(PCy$_3$)$_3$ even with a six-fold excess of PCy$_3$ [18]. Thus, the bis(triphenylphosphine)iminium salt [PPN$^+$] has been used to promote substitution by tertiary phosphines [51, 52]. The Ru$_3$(CO)$_9$(PCy$_3$)$_3$ was achieved by reactions of [PPN][Ru$_3$H(CO)$_{11}$] with PCy$_3$ in 1:5 ratio in methanol [53]. Another method of activating Ru$_3$(CO)$_{12}$ towards specific CO substitution is the use of a catalytic amount of [PPN][OAc] or [PPN][CN], which promotes substitution by tertiary phosphines such as PPh$_3$, dppm or dppe, but not by trialkyl phosphites or AsPh$_3$ [54]. This approach turned out to be successful for the synthesis of the Ru$_3$(CO)$_{10}$(μ-dppf) by a [PPN][OAc] catalyzed reaction between Ru$_3$(CO)$_{12}$ and the dppf ligand [17].

The trimethylamine oxide (Me$_3$NO) induced carbonyl substitutions also play an important role in the synthesis of many types of triruthenium cluster complexes [55]. The Ru$_3$(CO)$_{11}$(MeCN), Ru$_3$(CO)$_{10}$(MeCN)$_2$ and Ru$_3$(CO)$_9$(MeCN)$_3$ have been prepared from the reaction of Ru$_3$(CO)$_{12}$ with Me$_3$NO in the presence of a labile ligand such as acetonitrile. Thus, these new clusters have been shown to be convenient precursors in the preparation of other Ru$_3$ cluster types. For example, Ru$_3$(CO)$_{11}$(MeCN) reacts with one equimolar of PPh$_3$ to form Ru$_3$(CO)$_{11}$(PPh$_3$) [55] and three equimolars of Ru$_3$(μ-dppm)(CO)$_9$(η^1-dppa) with Ru$_3$(CO)$_9$(MeCN)$_3$ to

produce $Ru_3(CO)_9\{PPh_2C_2PPh_2Ru_3(\mu\text{-}dppm)(CO)_9\}_3$ [56]. It has also been shown that

the $Ru_3(CO)_7(SnPh_3)_2(\mu\text{-}SnPh_2)(\mu\text{-}dppm)(\mu\text{-}H)(\mu_3\text{-}H)]$ could be easily prepared from

treatment of $Ru_3(CO)_{10}(\mu\text{-}dppm)$ with two equivalents of Ph_3SnH in the presence of

Me_3NO [57].

In accordance with the improvement of these mild synthetic methods to

$Ru_3(CO)_{12}$ derivatives, significant interest in their chemistry has developed and many

complexes are thus known [48, 58]. The most common structural types of monodentate

(L') and bidentate (L–L) phosphine and arsine substituted $Ru_3(CO)_{12}$ are $Ru_3(CO)_{12-n}(L')_n$ [n = 1, 2, 3 and 4], $[Ru_3(CO)_{11}]_2(L–L)$, $Ru_3(CO)_{10}(L–L)$, $Ru_3(CO)_8(L–L)_2$ and

$Ru_3(CO)_9(L–L)(L')$ (Scheme 1.2) [59].
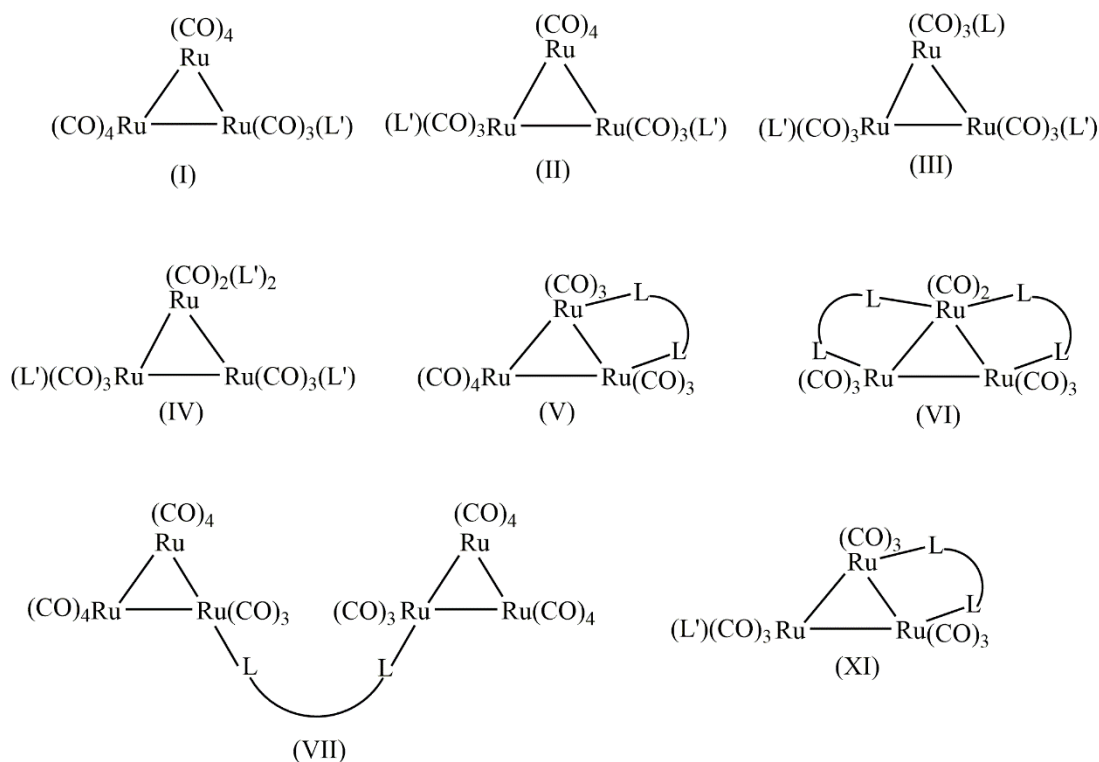
Scheme 1.2   Structural types of monodentate (L') and bidentate (L-L) phosphine and arsine substituted $Ru_3(CO)_{12}$. (I) $Ru_3(CO)_{11}(L')$; (II) $Ru_3(CO)_{10}(L')_2$; (III) $Ru_3(CO)_9(L')_3$; (IV) $Ru_3(CO)_8(L')_4$; (V) $Ru_3(CO)_{10}(L-L)$; (VI) $Ru_3(CO)_8(L-L)_2$; (VII) $[Ru_3(CO)_{11}]_2(L-L)$; (XI) $Ru_3(CO)_9(L-L)(L')$.

Bruce and his co-workers have described the stereochemistry of Group 8 metal carbonyls with Group 15 Ligands containing phosphine, arsine and phosphite substituted derivatives of $Ru_3(CO)_{12}$ [$Ru_3(CO)_{11}(L')$ (L' = $PPh(OMe)_2$, $P(OCH_2CF_3)_3$, $P(OCH_2)_3CEt$, $AsPh_3$) [60]; $Ru_3(CO)_{10}(L')_2$ (L' = PPh_3, $PPh(OMe)_2$, $P(OCH_2CF_3)_3$) [61]; $Ru_3(CO)_9(L')_3$ (L' = $PMe_2(CH_2Ph)$, PMe_2Ph, $AsMe_2Ph$, $PPh(OMe)_2$, $P(OEt)_3$, $P(OCH_2CF_3)_3$)[62]; $Ru_3(CO)_8(L')_4$ (L' = PMe_2Ph, $P(OMe)_3$, $P(OEt)_3$, $P(OPh)_3$) [63]]. These structural studies of monodentate phosphine, phosphite and arsine can be concluded in the following generalizations [63]: (1) Phosphine and arsine ligands preferably occupy equatorial coordination sites because of the steric reason. In di-, tri- and tetrasubstituted complexes, occupy positions which put each as far as possible from each other. (2) As the degree of substitution increases, so does the degree of distortion from D_{3h} symmetry in $Ru_3(CO)_{12}$ to D_3 symmetry by a twisting of the RuL_4 groups about the Ru-Ru bonds. (3) Substitution of group 15 ligand results in lengthening of the Ru-Ru bonds in $Ru_3(CO)_{11}(L')$ complexes and Ru-Ru bond *cis* to the ligand L' is affected the most. This lengthening correlate well with the size of the cone angles of the ligands. Bruce and co-workers did not observe any pronounced lengthening of such *cis* Ru-Ru bonds in $Ru_3(CO)_{10}(L')_2$ complexes, though the Ru_3 core expanded. (4) The average Ru-Ru distances increases with increasing degree of substitution, except in $Ru_3(\mu-CO)_2(CO)_6(PPh(OMe)_2)_4$ where there is a change in structure type. (5) The Ru-L distances correlated with the cone angles. Following this interest, the correlations of Ru-L bond lengths in triruthenium complexes with Tolman cone angle for the ligand was intensively examined [64-66].

Extensive single crystal X-ray structural studies have been undertaken for $Ru_3(CO)_{12-n}(L')_n$ where [n = 1, 2,3 and 4] have given exclusive knowledge of their structural features. The selected bond parameters for $Ru_3(CO)_{12-n}(L)_n$ where [n = 1, 2,

3 and 4] complexes are shown in Table 1.2. Triruthenium clusters with four substitutions of monodentate phosphine ligands [$Ru_3(CO)_8(L')_4$] have been the subject of very few reports although there are many available derivatives of the PR_3 ligands. To date, there are only five structural reports on [$Ru_3(CO)_8(L')_4$] complexes available in CSD database [67], namely $Ru_3(\mu\text{-}CO)_2(CO)_6(PPh(OMe)_2)_4$ [68] $Ru_3(CO)_8(PMe_2Ph)_4$, $Ru_3(CO)_8(P(OMe)_3)_4$, $Ru_3(CO)_8(P(OEt)_3)_4$ and $Ru_3(CO)_8(P(OPh)_3)_4$ [63]. The reason is that introducing more tertiary phosphine ligands into a Ru_3 cluster will gradually weaken the Ru-Ru bonds. However, the synthesis of this type of complexes had earlier been studied on $Ru_3(CO)_8(PH_3)_4$, obtained from a reaction between [$RuCl_2(CO)_3]_2$ and PH_3 [69], $Ru_3(CO)_{12-n}(PF_3)_n$ [n=4-6] [46], and $Ru_3(CO)_8(PMe_3)_4$ but no single crystal X-ray data has been reported [18].

The structure of $Ru_3(\mu\text{-}CO)_2(CO)_6(PPh(OMe)_2)_4$ is the first example of derivatives of $Ru_3(CO)_{12}$ with the $Fe_3(CO)_{12}$ type structure which adopts a structure with two carbonyls asymmetrically bridging the shorter Ru-Ru bond (2.797(1) Å) and the other two Ru-Ru bonds are identical at 2.879(1) Å [68]. The other [$Ru_3(CO)_8(L')_4$] [where L' = PMe_2Ph, $P(OMe)_3$, $P(OPh)_3$ and $P(OEt)_3$] complexes have structures shown in Scheme 1.2.

Table 1.2   Average Ru–Ru and Ru–L' bond lengths in complexes $Ru_3(CO)_{12-n}(L')_n$ [n = 1, 2, 3 and 4].

L'	Cone angle (°)	Ru–Ru (Å)				Ru–L (Å)				Ref.
		n = 1	2	3	4	1	2	3	4	
$AsPh_3$	142	2.868				2.464				[60]
$As(C_6H_4SMe\text{-}p)_3$	-	2.851				2.452				[70]
$As(p\text{-}Tol)_3$	-	2.862				2.463				[71]
$AsMe_2Ph$	125			2.845				2.444		[62]
PMe_2Ph	127			2.858		2.334				[62]
					2.866				2.257	[63]
$PMe_2(CH_2Ph)$	120			2.860				2.314		[62]
PPh_3	145	2.886				2.380				[45]
			2.842				2.357			[61]
				2.873				2.340		[72]
$P(p\text{-}Tol)_3$	145	2.856				2.346				[58]
$PPh_2(C_6F_5)$	-	2.864				2.343				[58]
$P(C_6H_4Cl\text{-}p)_3$	145	2.853				2.346				[58]
$P(C_6H_4Cl\text{-}m)_3$		2.874				2.359				[73]
			2.860				2.343			[74]
$P(C_6H_4F\text{-}m)_3$	-	2.877				2.364				[75]
				2.883				2.337		[75]
$P(C_6H_4F\text{-}p)_3$	145	2.856				2.349				[75]
			2.865				2.367			[75]
$P(3,5\text{-}CF_3\text{-}C_6H_3)_3$	-	2.847				2.334				[58]
$PPh_2(C_9H_8N)$	-	2.876				2.367				[76]
$PPh(C_9H_8N)_2$	-	2.852				2.359				[76]
$PPh_2(C_{17}H_{12}N_2)$	-	2.871				2.343				[76]
				2.939				2.414		[53]

Table 1.2   (Continued)

L'	Cone angle (°)	Ru–Ru (Å)				Ru–L (Å)				Ref.
		n = 1	2	3	4	1	2	3	4	
PCy$_3$	170	2.880				2.425				[77]
				2.939				2.414		[53]
P(OEt)$_3$	109	2.847				2.281				[78]
				2.855				2.292		[62]
					2.855				2.25	[63]
PCy$_2$(2-phenyl-1H-inden-3-yl)	-	2.886				2.411				[79]
PMe$_3$	118	2.852				2.356				[80]
				2.859				2.330		[81]
P(OMe)$_3$	107	2.877				2.275				[64]
			2.850				2.298			[64]
				2.854				2.280		[82]
					2.857				2.258	[63]
PEt$_3$	132	2.884				2.349				[64]
			2.862				2.351			[83]
P(OPh)$_3$	128	2.848				2.256				[84]
			2.850							[81]
					2.876				2.265	[63]
PPh(OMe)$_2$	115	2.883				2.288				[60]
			2.890				2.294			[61]
				2.886				2.284		[62]
					2.852				2.279	[68]
P(OCH$_2$)$_3$CEt	101	2.842				2.238				[68]

14

Table 1.2   (Continued)

L'	Cone angle (°)	Ru–Ru (Å)				Ru–L (Å)				Ref.
		n = 1	2	3	4	1	2	3	4	
P(OCH$_2$CF$_3$)$_3$	110	2.856				2.254				[68]
			2.846				2.250			[61]
				2.858				2.246		[62]
P(OCH$_2$CH$_2$Cl)$_3$	-	2.855				2.261				[85]
PTA	-	2.823				2.292				[39]
			2.849				2.299			[39]
				2.873				2.297		[39]
P(OPr^i)$_3$	130		2.847				2.289			[86]
				2.853				2.295		[86]
P(Me$_2$nap)	-		2.865				2.345			[87]
P(C$_4$H$_3$S)$_3$	-		2.942				2.352			[19]
PPh$_2$((CH$_2$)$_3$Ph)	-			2.867				2.332		[88]

Table 1.3   Ru–Ru bond lengths of some $Ru_3(CO)_{10}(L–L)$ and $Ru_3(CO)_8(L–L)_2$ complexes.

Complexes	L–L bridged	L–L unbridged	Ref.
$Ru_3(CO)_{10}(\mu\text{-dppm})$	2.834(1)	2.860(1), 2.841(1)	[35]
$Ru_3(CO)_8(\mu\text{-dppm})_2$	2.833(2), 2.826(2)	2.858(2)	[89]
$Ru_3(CO)_6(\mu\text{-dppm})_3$	2.862(1), 2.851(1) 2.851(1)		[90]
$Ru_3(CO)_{10}(\mu\text{-dpam})$	2.845(1)	2.840(1), 2.817(1)	[91]
$Ru_3(CO)_8(\mu\text{-dppm})(\mu\text{-dpam})$	2.850(2), 2.828(2)	2.848 (2)	
$Ru_3(CO)_{10}(\mu\text{-arphos})$	2.8532(6)	2.8331(6), 2.8512(6)	[92]
$Ru_3(CO)_{10}(\mu\text{-mapm})$	2.8464(3)	2.8567(3), 2.8504(3)	[93]
$Ru_3(CO)_{10}(\mu\text{-dppe})$	2.856(1)	2.847(1), 2.855(1)	[36]
$Ru_3(CO)_{10}(\mu\text{-F-dppe})$	2.8684(4)	2.8494(4), 2.8422(4)	[94]
$Ru_3(CO)_8(\mu\text{-F-dppe})_2$	2.8786(6)	2.9027(5), 2.8801(5)	[94]
$Ru_3(CO)_{10}(\mu\text{-dppee})$	2.836(1)	2.862(1), 2.840(1)	[95]
$Ru_3(CO)_{10}(\mu\text{-dppb})$	2.9053(2)	2.8448(1), 2.8507(2)	[96]
$Ru_3(CO)_{10}(\mu\text{-dpph})$	2.9531(2)	2.8842(2), 2.8876(2)	[41]
$Ru_3(CO)_{10}(\mu\text{-dppf})$	2.9284(5)	2.8600(4), 2.8600(4)	[17]
$Ru_3(CO)_{10}(\mu\text{-ffars})$	2.858(6)	2.831(3), 2.831(3)	[97]
$Ru_3(CO)_8(\mu\text{-ffars})_2$	2.853(3), 2.853(3)	2.785(4)	[98]
$Ru_3(CO)_{10}(\mu\text{-diop})$	2.888(1)	2.845(2), 2.836(2)	[99]
$Ru_3(CO)_{10}(\mu\text{-dcpm})$	2.8384(7)	2.8378(7), 2.8596(8)	[94]
$Ru_3(CO)_8(\mu\text{-dcpm})_2$	2.8572(5), 2.8718(6)	2.8357(6)	[94]
$Ru_3(CO)_{10}(\mu\text{-dpmb})$	2.9431(16)	2.9009(15), 2.8955(15)	[100]
$Ru_3(CO)_{10}(\mu\text{-dppa})$	2.8287(11)	2.8546(10), 2.8545(10)	[101]
$Ru_3(CO)_8(\mu\text{-dppa})_2$	2.823(2), 2.833(3)	2.8223(13)	[101]

For bidentate ligands, there are two different trends of the Ru-Ru bond distances as summarized in Table 1.3 but all phosphines and arsines occupy equatorial coordination sites. In $Ru_3(CO)_{10}(L\text{-}L)$ [where L–L = dppe, dppb, dpph] complexes, the bridged Ru-Ru bonds are longer than the unbridged ones. The bridged Ru-Ru bonds become longer as the number of methylene chain increases in bidentate ligands $[Ru_3(CO)_{10}(\mu\text{-dppe}) = 2.856(1)$ Å [36]; $Ru_3(CO)_{10}(\mu\text{-dppb}) = 2.9053(2)$ Å [96]; $Ru_3(CO)_{10}(\mu\text{-dpph}) = 2.9531(2)$ Å [41]]. The similar bridged Ru-Ru bonds are longer than the unbridged ones can be seen in $Ru_3(CO)_{10}(\mu\text{-F-dppe})$ [94], $Ru_3(CO)_{10}(\mu\text{-dppf})$ [17], $Ru_3(CO)_{10}(\mu\text{-diop})$ [99], $Ru_3(CO)_{10}(\mu\text{-arphos})$ [92] and $Ru_3(CO)_{10}(\mu\text{-dpmb})$ [100]. For $Ru_3(CO)_{10}(\mu\text{-dpam})$, the bridged Ru–Ru bond (2.845(1) Å) is slightly

longer than the unbridged Ru–Ru bonds (2.840(1) Å and 2.817(1) Å). The bridged Ru-Ru bonds are also longer than unbridged ones in $Ru_3(CO)_8(\mu\text{-dppa})_2$ [101], $Ru_3(CO)_8(\mu\text{-dcpm})_2$ [94] and $Ru_3(CO)_8(\mu\text{-ffars})_2$ [102]. In contrast, $Ru_3(CO)_{10}(\mu\text{-dppm})$ and $Ru_3(CO)_8(\mu\text{-dppm})_2$ show the unbridged Ru–Ru bonds are longer than the bridged bond as a result of the strain in the five membered chelate rings [35]. In fact, Ru–Ru bond spanned by dppm [2.828(2) Å] is shorter than that spanned by dpam [2.850(2) Å] and the non-bridged bond [2.848(2) Å] in $Ru_3(CO)_8(\mu\text{-dppm})(\mu\text{-dpam})$ [103]. As stated by Coleman and co-workers [35], there is some correlation between the value of intracyclic angles and the corresponding Ru–Ru bond length but the observation is having been made only on $Ru_3(CO)_{10}(\mu\text{-dppm})$ and $Ru_3(CO)_{10}(\mu\text{-ffars})$.

The first complex in which three bridging bidentate phosphine ligands are attached to Ru–Ru edge in μ-bridging mode is $Ru_3(CO)_6(\mu\text{-dppm})_3$. The synthesis of $Ru_3(CO)_6(\mu\text{-dppm})_3$ was first reported by Smith and co-workers [104] on heating $Ru_3(CO)_{12}$ and dppm in benzene for 8 h. Again, in a separate experiment, the single crystal X-ray data has been established but $Ru_3(CO)_6(\mu\text{-dppm})_3$ was a minor product from the reduction of ruthenium(III) acetate, prepared in situ from $RuCl_3.3H_2O$ and silver acetate, with $NaBH_4$ in the presence of dppm and CO [90]. The distance of the bridged Ru–Ru bonds [2.862(1), 2.851(1), 2.851(1) Å] are not different from those in $Ru_3(CO)_{12}$ [2.8595(4), 2.8512(4), 2.8518(4) Å] [16]. $Ru_3(CO)_6(\mu\text{-dppm})_3$ can be oxidized by silver(I) and oxygen or Me_3NO to yield the oxo-capped cluster $[Ru_3(\mu_3\text{-}O)(\mu_3\text{-CO})(CO)_3(\mu\text{-dppm})_3]$ which also undergoes reversible protonation to give the related hydroxide cluster $[Ru_3(\mu_3\text{-OH})(\mu_3\text{-CO})(CO)_3(\mu\text{-dppm})_3]^+$ (Scheme 1.3) [105].

Ph$_2$P—————PPh$_2$

Ph$_2$P——Ru————Ru——PPh$_2$
       (CO)$_2$ (CO)$_2$
       P——Ru——P
      Ph$_2$ (CO)$_2$ Ph$_2$

Ru$_3$(CO)$_6$(μ-dppm)$_3$

$\xrightarrow{\text{Me}_3\text{NO}}$

Ph$_2$P—————PPh$_2$
                O
Ph$_2$P——Ru————Ru——PPh$_2$
       (CO)   (CO)
       P——Ru——P
      Ph$_2$ (CO) Ph$_2$
              C
              O

Ru$_3$(μ_3-O)(μ_3-CO)(CO)$_3$(μ-dppm)$_3$

$-H^+$ $\updownarrow$ H^+

Ph$_2$P—————PPh$_2$ $\oplus$
            H
            O
Ph$_2$P——Ru————Ru——PPh$_2$
       (CO)   (CO)
       P——Ru——P
      Ph$_2$ (CO) Ph$_2$
              C
              O

[Ru$_3$(μ_3-OH)(μ_3-CO)(CO)$_3$(μ-dppm)$_3$]$^+$
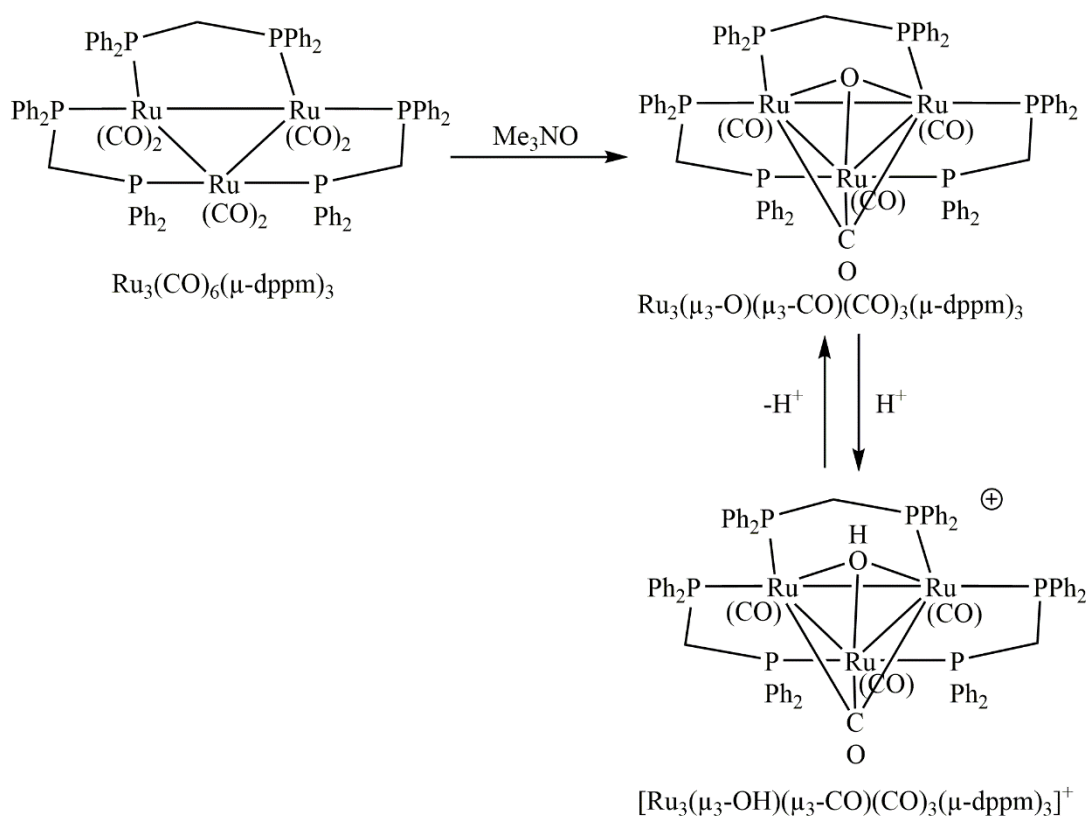
Scheme 1.3   Formation of oxo-cluster from Ru$_3$(CO)$_6$(μ-dppm)$_3$.

The structures of [Ru$_3$(CO)$_{11}$]$_2$(dppe), [Ru$_3$(CO)$_{11}$]$_2$(DBP) [106] and [Ru$_3$(CO)$_{11}$]$_2$(dppf) [107] are the only few complexes known with phosphine ligands connecting two cluster units. In [Ru$_3$(CO)$_{11}$]$_2$(dppe), the Ru–Ru bonds *cis* to the phosphine at 2.891(1) Å is longer than other Ru–Ru bonds which average 2.855 Å [106]. The other Ru$_3$ analogues of these types have the same structure as [Ru$_3$(CO)$_{11}$]$_2$(dppe) and the Ru–Ru bonds have similar trends.

Although the basic type of triruthenium Ru$_3$(CO)$_{12-n}$(L')$_n$ [n = 1, 2, 3 and 4], Ru$_3$(CO)$_{10}$(L-L), Ru$_3$(CO)$_8$(L-L)$_2$, [Ru$_3$(CO)$_{11}$]$_2$(L-L), Ru$_3$(CO)$_9$(L-L)(L') phoshine complexes were established at much the same time as those of the arsine analogues, there is still no crystallographic data reported on Ru$_3$(CO)$_{10}$(L-L) [where L-L = dppp and dpppe], Ru$_3$(CO)$_8$(L-L)$_2$ [where L-L = dpam, dppe, dppp, dpppe, dpph] and

$[Ru_3(CO)_{11}]_2$(L-L) [where L-L = dppp, dppb, dpppe, dpph]. Only precise X-ray structural data can provide certainty over metal complex geometry structure, identity, and dimensions, which support the bonding types and the overall understanding in this type of complexes.

A further feature of interest in the chemistry of Group 15 ligands with a triruthenium cluster is $Ru_3(CO)_9$(L–L)(L') complexes [where L–L = bidentate ligand; L' = monodentate] is shown in Table 1.4. In all cases, the monodentate ligand is attached to the previously unsubstituted Ru atom and coordinated in the equatorial plane. There are two short Ru-Ru bonds and one relatively long Ru-Ru bond lying next to the introduced ligand. The difference between these bond lengths appears to correlate with the steric hindrance of the introduced ligand, with larger ligands inducing the greatest lengthening.
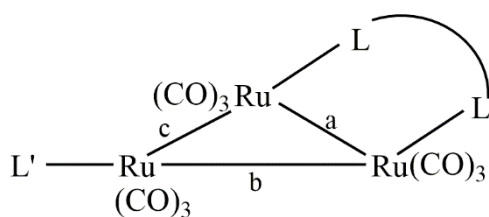
(CO)$_3$Ru

L

L

c a

L' —— Ru ———— Ru(CO)$_3$
(CO)$_3$ b

Table 1.4   Selected bond lengths of Ru$_3$(CO)$_9$(L-L)(L') complexes.

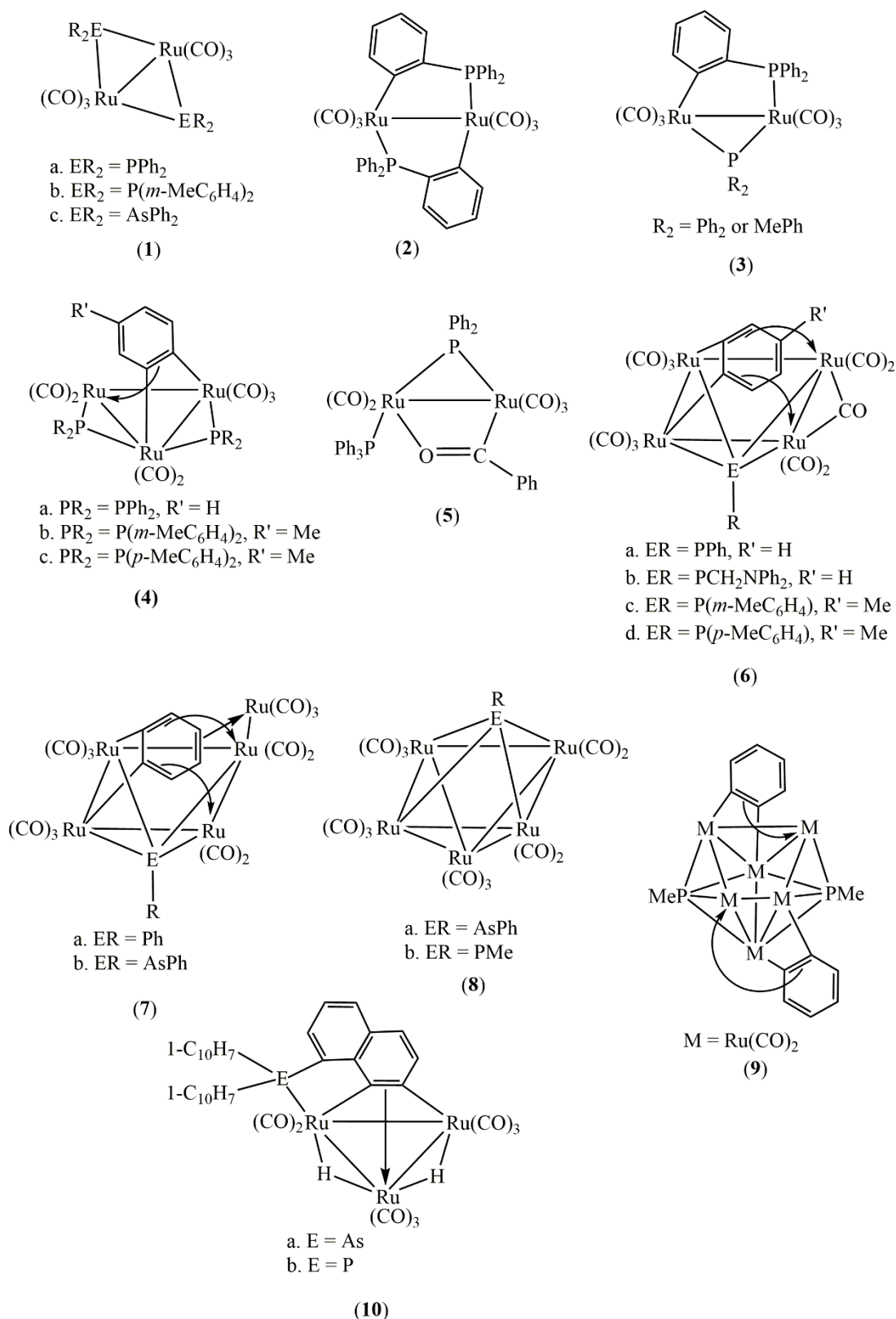| L-L	L'	Ru–Ru (Å)			Ru–L'	Ref.
		a	B	c		
dppm	SbPh$_3$	2.8518(6)	2.8533(6)	2.9030(6)	2.5925(5)	[108]
dppm	AsPh$_3$	2.8461(7)	2.8495(7)	2.8930(6)	2.4578(8)	[109]
dppm	As(PhSMe)$_3$	2.8428(18)	2.8183(19)	2.8975(18)	2.4534(2)	[110]
dppm	As(C$_6$H$_4$Me-p)$_3$	2.8338(2)	2.8208(2)	2.8890(2)	2.4706(2)	[111]
dppm	As(PhOMe)$_3$	2.8384(13)	2.8294(14)	2.8935(13)	2.4458(16)	[112]
dppm	PCy$_3$	2.8476(8)	2.8587(8)	2.9060(9)	2.397(2)	[66]
dppm	PPh$_3$	2.835(1)	2.8592(9)	2.8697(9)	2.360(2)	[66]
dppm	PPr$^i_3$	2.8756(3)	2.8586(5)	2.9076(4)	2.3852(8)	[66]
dppm	PPh$_2$(PhCHO)	2.8343(9)	2.8541(9)	2.899(1)	2.359(2)	[66]
dppm	P(OCH$_3$)$_3$	2.8515(4)	2.8473(4)	2.8760(3)	2.2642(8)	[113]
dppm	PPh$_2$(C$_2$PPh$_2$)	2.8229(3)	2.8329(4)	2.8530(3)	2.3176(9)	[56]
dppm	PPh$_2$(CH$_2$SPh)	2.8449(8)	2.8352(8)	2.8743(8)	2.3288(13)	[114]
dppm	P(C$_4$H$_3$S)$_3$	2.8523(3)	2.8622(3)	2.8938(3)	2.3374(8)	[115]
dpam	PPh$_2$(PhSCH$_3$)	2.8522(3)	2.8357(3)	2.8606(3)	2.3453(7)	[116]
dpam	As(PhOMe)$_3$	2.8587(16)	2.8170(16)	2.8809(16)	2.4460(19)	[117]
dpam	AsPh(PhOMe)$_2$	2.8469(4)	2.8376(4)	2.8883(4)	2.3511(10)	[118]
dpam	AsPh$_2$(CH$_2$SPh)	2.8598(6)	2.8478(6)	2.8702(6)	2.3415(14)	[119]
dpam	As(C$_6$H$_4$Ph)$_3$	2.8590(7)	2.8153(7)	2.8767(10)	2.4641(8)	[120]
dpam	SbPh$_3$	2.8661(6)	2.8354(6)	2.8838(6)	2.5847(5	[121]
dpam	PPh$_3$	2.8652(2)	2.8560(2)	2.8809(2)	2.3641(5)	[109]
dpam	PCy$_3$	2.8699(5)	2.8621(5)	2.8769(5)	2.3905(14)	[122]
dpam	PPh$_2$C$_6$F$_5$	2.8653(3)	2.8418(3)	2.8730(3)	2.3367(7)	[123]
dpam	PPh$_2$(PhBr)	2.8495(5)	2.8366(5)	2.8870(6)	2.3423(13)	[124]
dpam	P(p-Tol)$_3$	2.8539(4)	2.8460(4)	2.8790(4)	2.3513(10)	[125]
dpam	P(OPr^i)$_3$	2.8780(16)	2.8106(15)	2.9092(15)	2.2926(4)	[126]
dpam	P(C$_6$H$_4$F-p)$_3$	2.8507(2)	2.8392(2)	2.8745(2)	2.3334(5)	[127]
dpam	PPh$_2$(PhSCH$_3$)	2.8493(2)	2.8463(2)	2.9094(2)	2.3612(6)	[128]
dotpm	P(OPh)$_3$	2.8557 (2)	2.8473 (2)	2.8510 (2)	2.2488 (5)	[129]
dotpm	P(OCH$_2$CH$_2$Cl)$_3$	2.8492 (2)	2.8415 (2)	2.8614 (2)	2.2543 (5)	[130]
dotpm	P(C$_6$H$_4$Cl-p)$_3$	2.8547(3)	2.8634(3)	2.8750(3)	2.3418(8)	[131]
dotpm	PPh$_2$(C$_6$H$_4$Br)	2.8621(3)	2.8533(3)	2.8948(3)	2.3399(7)	[131]
dpbm	PTh$_3$	2.8585(4)	2.8351(4)	2.8868(3)	2.3261(8)	[132]
dppe	SbPh$_3$	2.8651(5)	2.8124(5)	2.8676(5)	2.5846(4)	[133]
dppe	As(C$_6$H$_4$OMe)$_3$	2.8439(4)	2.8221(4)	2.8694(5)	2.4558(5)	[134]

1.4 Thermolysis reactions of some triruthenium phosphine and arsine complexes

Thermolysis reaction is also sometimes known as pyrolysis reaction. Thermolysis has been used in the preparation of high nuclearity triruthenium carbonyl clusters. Thermolysis generally involves heating the reaction between a transition metal carbonyl cluster containing the appropriate ligand or complexes at certain temperatures. The products, obtained from this reaction, mainly depends on both the solvent and reaction conditions [1]. Some of the earliest thermolysis of triruthenium complexes containing tertiary phosphine or arsine ligands often lead to C–H and/or P/As–C(Ph) bond cleavages and formation of new M–P or M–C bonds [46]. Generally, the observed results are orthometallation of a Ph group to give $PR_2(C_6H_4)$ or $PR(C_6H_4)$ ligands or the formation of phosphido complexes with related loss of the Ph group (probably as benzene) by combination with a cluster hydride or the ortho-H atom [135, 136]. The activation of alkyl C–H bond in coordinated phosphine ligands give rise to cyclometallation products which formed a chelate ring containing M–C bond [137-139]. Subsequently, thermolysis is also one of the methods of preparing aryne derivatives of a metal cluster which are formed by combination of C–H and P–C bond cleavage reactions to produce the benzyne cluster [140].

The initial thermolysis studies on the triruthenium cluster were conducted on the series of $Ru_3(CO)_9(PR_3)_3$ complexes [PR_3 = PPh_3, $P(m\text{-}Me(C_6H_4)_3)$, $P(p\text{-}Me(C_6H_4)_3)$, $PMePh_2$]. These complexes, treated in refluxing decalin resulted in the formation of binuclear complexes [$Ru_2(CO)_6(PPh_2)_2$ (**1a**), $Ru_2(CO)_6(P(m\text{-}Me(C_6H_4)_2)$ (**1b**), $Ru_2(CO)_6(PPh_2(C_6H_4))_2$ (**2**), $Ru_2(CO)_6(PR_2(C_6H_4))(PR_2)$ [R_2= Ph or MePh] (**3**) and benzyne complexes [**4a-4c**] [46]. The formation of (**3**) results from two aryl C–H cleavages while (**2**) forms from one aryl C–H and one aryl C–P cleavages. In another

21

observation, treating $Ru_3(CO)_9(PPh_3)_3$ in refluxing toluene also affords the binuclear acyl (**5**) and benzyne (**4a**) complex [141]. Complex (**5**) results from one aryl C–P cleavage and a CO insertion to a phenyl group. It is interesting to note that C–P cleavages in (**5**) can take place without C–H cleavage. Products of the thermolysis of some of triruthenium clusters containing monodentate Group 15 ligands are shown in Scheme 1.4. The formation of several binuclear products for Ru_3 compared to Os_3 cluster in these studies reflect that the Ru–Ru bonds is weaker than the Os–Os bonds. There is also no formation of ruthenium hydride species in contrast to the such complexes observed in the triosmium system (Scheme 1.5). For example, thermolysis of $Os_3(CO)_{10}(PPh_3)_2$ affords complexes $Os_3(CO)_8(\mu\text{-}H)(PPh_3)(PPh_2C_6H_4)$ (**11**), $Os_3(CO)_9(\mu\text{-}H)(PPh_3)(PPh_2C_6H_4)$ (**12**), $Os_3(CO)_8(PPh_2)(Ph)(PPhC_6H_4)$ (**13**) and three benzyne complexes $Os_3(CO)_7(PPh_2)_2(C_6H_4)$ (**14**), $Os_3(CO)_7(\mu\text{-}H)(PPh_2)(PPh_3)(C_6H_4)$ (**15**) and $Os_3(CO)_7(\mu\text{-}H)(PPh_2)(PPh_2C_6H_4C_6H_3)$ (**16**) [142, 143].

Thermolysis of $Ru_3(CO)_{11}(PPh_3)$ in toluene for 18 h affords three benzynes complexes $[Ru_3(CO)_7(\mu\text{-}PPh_2)_2(\mu_3\text{-}\eta^2\text{-}C_6H_4)$ (33%) (**4a**), $[Ru_4(CO)_{10}(\mu\text{-}CO)(\mu_4\text{-}PPh)(\mu_4\text{-}\eta^4\text{-}C_6H_4)]$ (50%) (**6a**) and $[Ru_5(CO)_{13}(\mu_4\text{-}PPh)(\mu_5\text{-}\eta^6\text{-}C_6H_4)]$ (7%) (**7a**) [140, 144]. The formation of $Ru_3(CO)_7(\mu\text{-}PPh_2)_2(\mu_3\text{-}\eta^2\text{-}C_6H_4)$ (**4a**) from $Ru_3(CO)_{11}(PPh_3)$ involves two aryls C–P and one aryl C–H cleavages with a rearrangement of the phosphine ligand.   Likewise, thermolysis of $Ru_3(CO)_{11}(PPh_2CH_2NPh_2)$ and $Ru_3(CO)_{11}(PPh_2Me)$ gives $Ru_6(CO)_{12}(\mu_4\text{-}PMe_2)(\mu_3\text{-}\eta^2\text{-}C_6H_4)_2$ (**9**) and $Ru_4(CO)_{10}(\mu\text{-}CO)(\mu_4\text{-}PMe)(\mu_4\text{-}\eta^4\text{-}C_6H_4)]$ (**6c**), respectively [140, 144]. Thermal transformation of $Ru_3(CO)_{11}(PPh_2Me)$ in refluxing octane is radically altered leading to different reaction products; $Ru_5(CO)_{15}(\mu_4\text{-}PMe)$ (**8b**) and $Ru_6(CO)_{12}(\mu_4\text{-}PMe_2)(\mu_3\text{-}\eta^2\text{-}C_6H_4)_2$ (**9**) [140]. A better yield (60%) of (**4a**) obtained when $Ru_3(CO)_{10}(PPh_3)_2$ is heated in toluene for 2.5 h, but no (**6a**) and (**7a**) is produced under these conditions [140].

(1)

a. $ER_2 = PPh_2$
b. $ER_2 = P(m\text{-}MeC_6H_4)_2$
c. $ER_2 = AsPh_2$

(2)

(3)

$R_2 = Ph_2$ or MePh

(4)

a. $PR_2 = PPh_2$, R' = H
b. $PR_2 = P(m\text{-}MeC_6H_4)_2$, R' = Me
c. $PR_2 = P(p\text{-}MeC_6H_4)_2$, R' = Me

(5)

(6)

a. $ER = PPh$, R' = H
b. $ER = PCH_2NPh_2$, R' = H
c. $ER = P(m\text{-}MeC_6H_4)$, R' = Me
d. $ER = P(p\text{-}MeC_6H_4)$, R' = Me

(7)

a. $ER = Ph$
b. $ER = AsPh$

(8)

a. $ER = AsPh$
b. $ER = PMe$

(9)

$M = Ru(CO)_2$

(10)

a. $E = As$
b. $E = P$

Scheme 1.4   Products of the thermolysis of some of triruthenium clusters containing monodentate Group 15 ligands.

23

The analogous complexes (**4b**) and (**4c**) were also obtained from the thermolysis of $Ru_3(CO)_{11}(PR_3)$ (R= m-MeC_6H_4, p-MeC_6H_4) in refluxing decalin or mesitylene together with the tetraruthenium benzyne complexes $Ru_4(CO)_{10}(\mu$-$CO)(\mu_4$-$C_6H_4R')(\mu_4$-PR) (R' = Me, R = m-MeC_6H_4 (**6d**); R' = Me, R = p-MeC_6H_4) (**6e**) [46]. Thermolysis of $Ru_3(CO)_{11}(AsPh_3)$ gives high yields of $Ru_2(CO)_6(AsPh_2)_2$ (**1c**) and minor products of pentanuclear complexes $Ru_5(CO)_{13}(\mu_4$-$AsPh)(\mu_5$-η^6-$C_6H_4)$ (**7b**) and $Ru_5(CO)_{13}(\mu_4$-$AsPh)(\mu_5$- η^6-$C_6H_4)$ (**8a**) [140].

Heating $Ru_3(CO)_{12}$ and $As(1$-$C_{10}H_7)_3$ [tris(1-naphtyl)arsine] in cyclohexane for 10 hours results in the formation $Ru_3(CO)_8(\mu$-$H)_2[\mu_3$-η^4-$(C_{10}H_7)_2As(C_{10}H_5)]$ (**10a**) while with $P(1$-$C_{10}H_7)_3$ for 24 hours was also yielded similar products of $[Ru_3(CO)_8(\mu$-$H)_2[\mu_3$-η^4-$(C_{10}H_7)_2P(C_{10}H_5)$ (**10b**). Both complexes were reported as the first naphtyne of triruthenium cluster to be isolated and derived from double metallation of the unsubstituted aromatic rings [145].
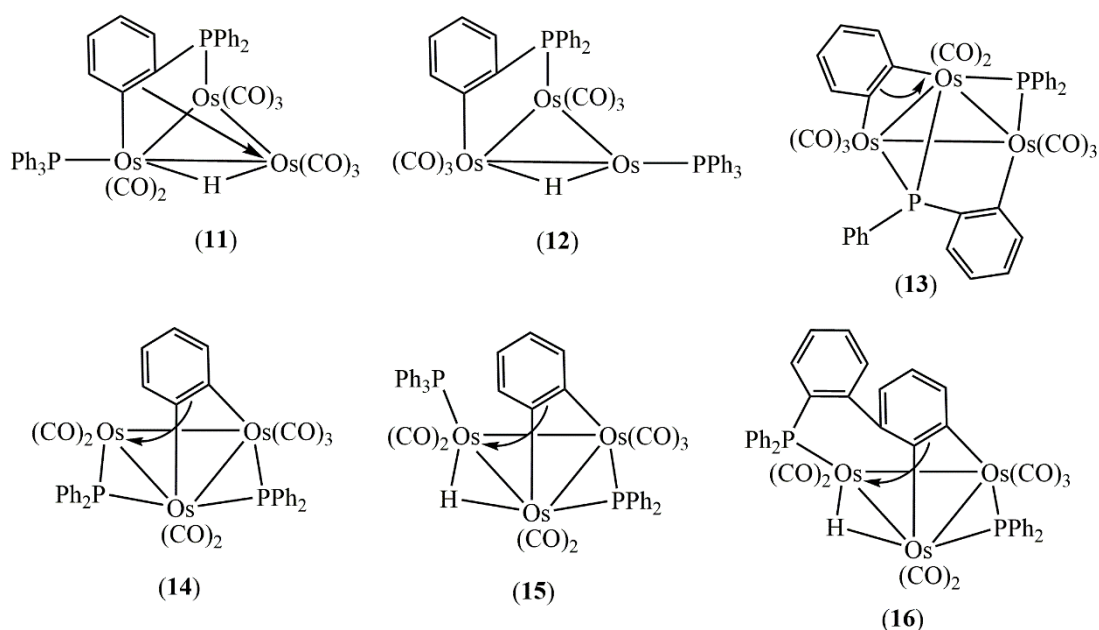
Scheme 1.5   Products of the thermolysis of some triosmium cluster containing monodentate Group 15 ligands.